

Mixing, strong and radiative decays of the scalars $f_0(980)$ and $a_0(980)$ in a hadronic molecule approach.

Tanja Branz, Thomas Gutsche, Valery E. Lyubovitskij *

*Institut für Theoretische Physik, Universität Tübingen,
Auf der Morgenstelle 14, D-72076 Tübingen, Germany*

(Dated: May 29, 2019)

We analyze the influence of $a_0 - f_0$ -mixing effects on the electromagnetic and strong decay properties of the light scalars $a_0(980)$ and $f_0(980)$ within a hadronic molecule interpretation. Both scalars are discussed within a covariant and gauge invariant model which also allows for finite size effects due to their spatially extended structure in the $K\bar{K}$ -bound state picture. Allowing for $a_0 - f_0$ mixing we study the radiative decays $f_0/a_0 \rightarrow \gamma\gamma$, $f_0/a_0 \rightarrow \gamma\omega$ and $f_0/a_0 \rightarrow \gamma\rho$ as well as the ϕ -production of the f_0 and a_0 with respect to finite size effects and variations of the mixing angle. Furthermore, we apply our formalism to describe the strong $f_0 \rightarrow \pi\pi$ and $a_0 \rightarrow \pi\eta$ decay properties.

PACS numbers: 13.25.Jx,13.40.Hq,36.10Gv

Keywords: scalar mesons, hadronic molecules, relativistic meson model, electromagnetic and strong decays

arXiv:0808.0705v1 [hep-ph] 5 Aug 2008

* On leave of absence from the Department of Physics, Tomsk State University, 634050 Tomsk, Russia

I. INTRODUCTION

Until now meson spectroscopy provides a valuable tool to explore the structure and properties of mesons and, extending the scope, to get further information on the confinement regime of strong interaction. During the last decade, the meson mass spectrum showed a richer structure than might be expected from the constituent quark model which decisively influenced our understanding of hadronic structure in the past. In particular, the structure issue of the lightest scalars has been under permanent discussion concerning mesonic structure beyond the quark-antiquark picture. There exist different approaches concerning the substructure of the $f_0(980)$ and its 'twin' the $a_0(980)$ which range from $q\bar{q}$ [1, 2, 3] to tetraquark $q^2\bar{q}^2$ [4, 5, 6] interpretations. In [7] the structure of the light scalar nonet including $f_0(980)$ was tested using radiative ϕ decays. The authors of Ref. [7] point out the difficulty to distinguish between the $q\bar{q}$ and the $qq\bar{q}\bar{q}$ picture for the light scalar mesons. A possible admixture between $\bar{q}q$ and $qq\bar{q}\bar{q}$ configurations for the low-lying scalar mesons has been considered in Ref. [8] using the chiral approach. Both scalars are also discussed in a clustered version of the tetraquark configuration where the two quarks and antiquarks form a bound state of mesons - hadronic molecules [9, 10, 11].

In addition, an isospin violating mixture of the $f_0(980)$ and $a_0(980)$ mesons has been taken into consideration [12, 13, 14] which provides an interesting possibility to study its substructure. $f_0 - a_0$ mixing is on the one hand motivated by their near degenerate masses, on the other hand by the mass gap between the nearby charged and neutral $K\bar{K}$ thresholds.

In the present paper, the $f_0(980)$ and $a_0(980)$ mesons are treated as pure bound states of kaons. In order to describe the hadronic molecules we apply a theoretical framework which was successfully used in [15, 16, 17, 18, 19] and which is characterized by Lorentz- and gauge invariance. With particular consideration of the $f_0 - a_0$ mixing effects we discuss the electromagnetic decays with the final states occupied by photons and massive vector mesons $S \rightarrow V\gamma$, $S \rightarrow \gamma\gamma$ and $\phi \rightarrow S\gamma$, where $S = f_0, a_0$ and $V = \rho, \omega$, as well as the strong $a_0/f_0 \rightarrow \pi\pi/\pi\eta$ decay properties. In addition, the extended structure of mesonic bound states are also taken into consideration with a minimal amount of assumptions.

The framework we use for the mesonic molecule description of the a_0 and f_0 is shortly presented in the next section, in which we also address the issue of finite size and $a_0 - f_0$ -mixing effects. In sections III and IV we apply our model to the electromagnetic and strong decays and analyze the influence of mixing and the extended meson structure on the $a_0(980)$ and $f_0(980)$ decay properties. Our results are presented in section V, which we also compare with other approaches and with experimental data.

II. SETUP OF THE MODEL

The theoretical framework we use for our analysis is based on the nonlocal strong Lagrangians [15, 16, 17, 18, 19]

$$\begin{aligned}\mathcal{L}_{f_0 K\bar{K}} &= \frac{g_{f_0 K\bar{K}}}{\sqrt{2}} f_0(x) \int dy \Phi(y^2) \bar{K}\left(x - \frac{y}{2}\right) K\left(x + \frac{y}{2}\right), \\ \mathcal{L}_{a_0 K\bar{K}} &= \frac{g_{a_0 K\bar{K}}}{\sqrt{2}} \bar{a}_0(x) \int dy \Phi(y^2) \bar{K}\left(x - \frac{y}{2}\right) \vec{\tau} K\left(x + \frac{y}{2}\right),\end{aligned}\tag{1}$$

describing the interaction between the kaon-antikaon bound state and its constituents. The kaon and scalar fields are collected in the kaon isospin doublets and the scalar meson triplet

$$K = \begin{pmatrix} K^+ \\ K^0 \end{pmatrix}, \quad \bar{K} = \begin{pmatrix} K^- \\ \bar{K}^0 \end{pmatrix} \quad \text{and} \quad \bar{a}_0 = (a_0^+, a_0^0, a_0^-).\tag{2}$$

The vector $\vec{\tau} = (\tau^+, \tau^0, \tau^-)$ is characterized by the Pauli-matrices $\tau_{i=1,2,3}$, where $\tau^\pm = \frac{1}{\sqrt{2}}(\tau_1 \pm i\tau_2)$ and $\tau^0 = \tau_3$.

Finite size effects are incorporated in our model by the correlation function $\Phi(y^2)$. Its Fourier transform $\tilde{\Phi}(k_E^2)$ is directly related to the shape and size of the hadronic molecule and shows up as the form factor in the Feynman diagrams. Here, we employ a Gaussian form

$$\Phi(y^2) = \int \frac{d^4 k}{(2\pi)^4} \tilde{\Phi}(-k^2) e^{-iky} \quad \text{with} \quad \tilde{\Phi}(k_E^2) = \exp(-k_E^2/\Lambda^2),\tag{3}$$

where the index E refers to the Euclidean momentum space. The size parameter Λ controls the spatial extension of the hadronic molecule and is varied around 1 GeV. In the special case of point-like interaction, which we refer to as the local case, the correlation function $\Phi(y^2)$ is replaced by the delta-function $\lim_{\Lambda \rightarrow \infty} \Phi(y^2) = \delta^{(4)}(y)$.

The couplings to the constituent kaons, $g_{SK\bar{K}}$ with $S = f_0, a_0$, are determined self-consistently within our model by using the compositeness condition. It provides a method to fix the coupling strength between a bound state and its constituents [20, 21], therefore reduces the amount of free input parameters and also allows for a clear and straightforward determination of the decay properties. Note that this condition has also been used in the $K\bar{K}$ molecule approach in [10, 22]. The coupling constant can be easily extracted from the definition of the field renormalization constant Z_{f_0} which is set to zero

$$Z_S = 1 - \tilde{\Pi}'(m_{f_0}^2) = 0. \quad (4)$$

Here, $\tilde{\Pi}'(m_{f_0}^2) = \frac{g_{f_0 K \bar{K}}^2}{(4\pi)^2} \tilde{\Sigma}'(m_{f_0}^2)$ is the derivative of the mass operator with the kaon loop integral

$$\Sigma(p^2) = \int \frac{d^4 k}{\pi^2 i} \tilde{\Phi}^2(-k^2) S\left(k + \frac{p}{2}\right) S\left(k - \frac{p}{2}\right). \quad (5)$$

In general, meson loop diagrams are evaluated by using the free meson propagators given by

$$i S_K(x-y) = \langle 0 | T K(x) K^\dagger(y) | 0 \rangle = \int \frac{d^4 k}{(2\pi)^4 i} e^{-ik(x-y)} \tilde{S}_K(k), \quad (6)$$

in case of scalar and pseudoscalar mesons, where

$$\tilde{S}_K(k) = \frac{1}{m_K^2 - k^2 - i\epsilon}. \quad (7)$$

For vector and axialvector fields we use

$$i S_{M^*}^{\mu\nu}(x-y) = \langle 0 | T M^{*\mu}(x) M^{*\nu\dagger}(y) | 0 \rangle = \int \frac{d^4 k}{(2\pi)^4 i} \exp(-ik(x-y)) \tilde{S}_{M^*}^{\mu\nu}(k) \quad (8)$$

with

$$\tilde{S}_{M^*}^{\mu\nu}(k) = \frac{-g^{\mu\nu} + k^\mu k^\nu / m_{M^*}^2}{m_{M^*}^2 - k^2 - i\epsilon}. \quad (9)$$

Inclusion of $f_0 - a_0$ -mixing

Before we turn to the isospin violating $f_0 - a_0$ -mixing, we first shortly address the situation of exact isospin symmetry. In this case the light quark masses would be degenerate $m_u = m_d$ which leads to equal charged and neutral kaon masses $m_K \equiv m_{K^+} = m_{K^0}$ excluding electromagnetic corrections. Because of this reason, the off-diagonal elements of the transition amplitude $\langle a_0; I=1 | f_0; I=0 \rangle$ generated by kaon loops would vanish since the contributions from the charged and neutral kaons would cancel each other.

In reality of course, $SU(3)$ symmetry is broken and the light quark masses and hence the kaon masses split up. At this stage, isospin violating $a_0 - f_0$ -mixing might be caused on the one hand by the transition via charged and neutral kaon loops, which do not cancel because of $m_{K^\pm} \neq m_{K^0}$, but also by other mechanisms such as photon exchange (see Fig. 1) and isospin violating couplings [13]. Since not all mixing effects are unambiguously known, in the present

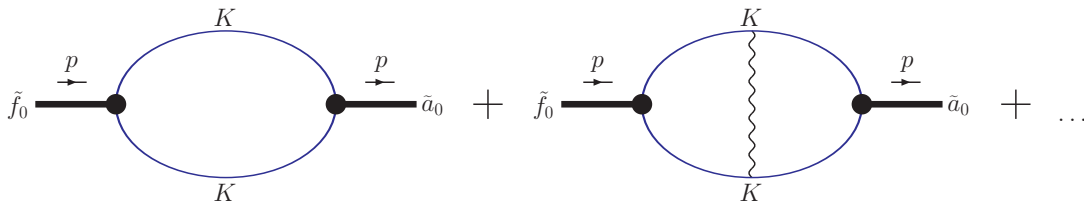


FIG. 1: $a_0 - f_0$ -mixing

analysis the mixing term $\delta m^2 f_0 a_0$, combining all contributions to the off-diagonal element in the Lagrangian $\tilde{\mathcal{L}}$, is

treated as a free parameter. At this intermediate 'bare' or 'unmixed' stage, the full effective Lagrangian of the bare \tilde{f}_0 and \tilde{a}_0 mesons and the constituent kaons can be written as

$$\begin{aligned} \mathcal{L} = & -\frac{1}{2}\tilde{f}_0(\square + \tilde{m}_{f_0}^2)\tilde{f}_0 - \frac{1}{2}\tilde{a}_0(\square + \tilde{m}_{a_0}^2)\tilde{a}_0 + \tilde{g}_{f_0 K \bar{K}}\tilde{f}_0\mathcal{J}_{f_0} + \tilde{g}_{a_0 K \bar{K}}\tilde{a}_0\mathcal{J}_{a_0} + \delta m^2\tilde{f}_0\tilde{a}_0 \\ & - K^+(\square + m_{K^\pm}^2)K^- - K^0(\square + m_{K^0}^2)\bar{K}^0, \end{aligned} \quad (10)$$

where the currents are given by $\mathcal{J}_{f_0} = \frac{K^+K^- + K^0\bar{K}^0}{\sqrt{2}}$, $\mathcal{J}_{a_0} = \frac{K^+K^- - K^0\bar{K}^0}{\sqrt{2}}$ and $m_{K^\pm} \neq m_{K^0}$. Due to the off-diagonal elements in the Lagrangian, the physical states $|f_0\rangle$ and $|a_0\rangle$ are obtained by applying the unitary transformation $U = \begin{pmatrix} \cos\theta & -\sin\theta \\ \sin\theta & \cos\theta \end{pmatrix}$ to the 'bare' basis $|\tilde{f}_0\rangle$ and $|\tilde{a}_0\rangle$ which diagonalizes the mass matrix

$$\mathcal{M} = U\tilde{\mathcal{M}}U^\dagger = U \begin{pmatrix} \tilde{m}_{f_0}^2 & \delta m^2 \\ \delta m^2 & \tilde{m}_{a_0}^2 \end{pmatrix} U^\dagger = \begin{pmatrix} m_{f_0}^2 & 0 \\ 0 & m_{a_0}^2 \end{pmatrix}. \quad (11)$$

The transformation U relates δm^2 to the mixing angle θ , where $m_{f_0}=0.98$ GeV and $m_{a_0}=0.9847$ GeV are the physical masses. The influence of mixing effects on the 'unmixed' or 'bare' masses \tilde{m}_{f_0} and \tilde{m}_{a_0} is demonstrated in Fig. 2, where \tilde{m}_{f_0} and \tilde{m}_{a_0} are plotted as functions of θ .

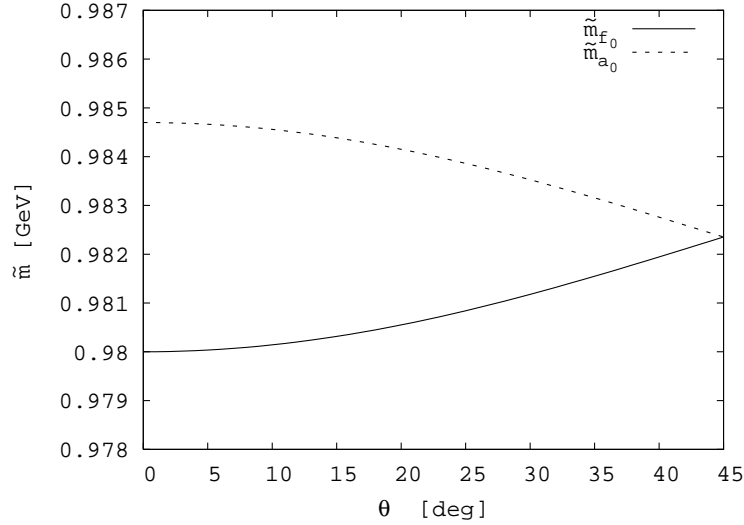


FIG. 2: Bare \tilde{f}_0 and \tilde{a}_0 masses in dependence on the $a_0 - f_0$ mixing-angle θ .

The interaction terms of the Lagrangian (10) expressed in terms of the physical scalars $f_0 = \tilde{f}_0 \cos\theta - \tilde{a}_0 \sin\theta$ and $a_0 = \tilde{a}_0 \cos\theta + \tilde{f}_0 \sin\theta$ read as

$$\begin{aligned} \mathcal{L}_{int} = & f_0 \left[(\tilde{g}_{f_0 K \bar{K}} \cos\theta - \tilde{g}_{a_0 K \bar{K}} \sin\theta) \frac{K^+K^-}{\sqrt{2}} + (\tilde{g}_{f_0 K \bar{K}} \cos\theta + \tilde{g}_{a_0 K \bar{K}} \sin\theta) \frac{K^0\bar{K}^0}{\sqrt{2}} \right] \\ & + a_0 \left[(\tilde{g}_{a_0 K \bar{K}} \cos\theta + \tilde{g}_{f_0 K \bar{K}} \sin\theta) \frac{K^+K^-}{\sqrt{2}} - (\tilde{g}_{a_0 K \bar{K}} \cos\theta - \tilde{g}_{f_0 K \bar{K}} \sin\theta) \frac{K^0\bar{K}^0}{\sqrt{2}} \right] \\ \equiv & f_0 \frac{g_{f_0 K^+ K^-}}{\sqrt{2}} K^+ K^- + f_0 \frac{g_{f_0 K^0 \bar{K}^0}}{\sqrt{2}} K^0 \bar{K}^0 + a_0 \frac{g_{a_0 K^+ K^-}}{\sqrt{2}} K^+ K^- + a_0 \frac{g_{a_0 K^0 \bar{K}^0}}{\sqrt{2}} K^0 \bar{K}^0 \end{aligned} \quad (12)$$

which defines the coupling strengths $g_{SK^+K^-}/\sqrt{2}$ and $g_{SK^0\bar{K}^0}/\sqrt{2}$ between the physical meson S and the charged or neutral kaon constituents in terms of the mixing angle θ and the bare couplings $\tilde{g}_{SK\bar{K}}$. We thereby determine the couplings $\tilde{g}_{SK\bar{K}}$ by using the compositeness condition as discussed above which, in the case of mixed states, leads to the system of equations

$$1 = \frac{1}{2}(\tilde{g}_{f_0 K \bar{K}}^2 \cos^2\theta + \tilde{g}_{a_0 K \bar{K}}^2 \sin^2\theta)(\Sigma^{0'}(p^2) + \Sigma^{\pm'}(p^2)) + \tilde{g}_{a_0 K \bar{K}}\tilde{g}_{f_0 K \bar{K}} \sin\theta \cos\theta(\Sigma^{0'}(p^2) - \Sigma^{\pm'}(p^2)) \Big|_{p^2=m_{f_0}^2} \quad (13)$$

$$1 = \frac{1}{2}(\tilde{g}_{a_0 K \bar{K}}^2 \cos^2\theta + \tilde{g}_{f_0 K \bar{K}}^2 \sin^2\theta)(\Sigma^{0'}(p^2) + \Sigma^{\pm'}(p^2)) - \tilde{g}_{a_0 K \bar{K}}\tilde{g}_{f_0 K \bar{K}} \sin\theta \cos\theta(\Sigma^{0'}(p^2) - \Sigma^{\pm'}(p^2)) \Big|_{p^2=m_{a_0}^2}, \quad (14)$$

where $\Sigma^{\pm\prime}(p^2)$ and $\Sigma^{0\prime}(p^2)$ denote the derivatives of the charged and neutral kaon loops already defined in Eq. (4). To circumvent the problem of a_0 inclusions in the mass operator of the f_0 we restrict to first order terms in $\delta \propto \delta m_K^2 = m_{K^0}^2 - m_{K^\pm}^2 \propto m_u - m_d$.

We study the influence of mixing effects on the scalar decay properties by writing the decay amplitude as sum of the interfering charged and neutral kaon loop contributions with the corresponding couplings $g_{SK^+K^-}$ and $g_{SK^0\bar{K}^0}$ defined in (12). However, for simplicity we do not indicate such a decomposition in the Feynman diagrams.

Of course, because of charge conservation only the neutral scalar a_0^0 undergoes mixing.

III. INCLUSION OF THE ELECTROMAGNETIC INTERACTION

The electromagnetic interaction terms are obtained by minimal substitution $\partial^\mu K^\pm \rightarrow (\partial^\mu \mp ieA^\mu)K^\pm$ in the free Lagrangian \mathcal{L}_K of charged kaons

$$\mathcal{L}_K = \partial_\mu K^+ \partial^\mu K^- - m_K^2 K^+ K^- \quad (15)$$

and the Lagrangians which couple vector mesons and kaons

$$\mathcal{L}_V = \sum_{V=\phi,\omega} \frac{g_{VK\bar{K}}}{\sqrt{2}} V^\mu (\bar{K} i \partial_\mu K - K i \partial_\mu \bar{K}) \quad (16)$$

and

$$\mathcal{L}_\rho = \frac{g_{VK\bar{K}}}{\sqrt{2}} \bar{\rho}^\mu (\bar{K} \vec{\tau} i \partial_\mu K - K \vec{\tau} i \partial_\mu \bar{K}), \quad (17)$$

respectively. The resulting electromagnetic interaction vertices are contained in the decay diagrams (a) and (b) of Figs. 3 and 4, and (a) to (c) of Fig. 5. In the local limit, the decay amplitude would be completely described by these Feynman diagrams. In contrast, the nonlocal strong interaction Lagrangians require special care in establishing gauge invariance. In doing so the charged fields are multiplied by exponentials [23] containing the electromagnetic field

$$K^\pm(y) \rightarrow e^{\mp ieI(y,x,P)} K^\pm(y) \quad (18)$$

with $I(y,x,P) = \int_x^y dz_\mu A^\mu(z)$, which gives rise to the electromagnetic gauge invariant Lagrangian

$$\mathcal{L}_{f_0 K \bar{K}}^{GI} = \frac{g_{f_0 K \bar{K}}}{\sqrt{2}} f_0(x) \int dy \Phi(y^2) [e^{-ieI(x+\frac{y}{2}, x-\frac{y}{2}, P)} K^+(x+\frac{y}{2}) K^-(x-\frac{y}{2}) + K^0(x+\frac{y}{2}) \bar{K}^0(x-\frac{y}{2})], \quad (19)$$

with a corresponding expression for the a_0 meson. The interaction terms up to second order in A^μ are obtained by expanding $\mathcal{L}_{f_0 K \bar{K}}^{GI}$ in terms of $I(y,x,P)$. Diagrammatically, the higher order terms give rise to nonlocal vertices with additional photon lines attached. The Feynman rules for these vertices have been already derived in [17]. Altogether, we obtain further graphs (Fig. 3 (c), (d) and (e)) governing the two-photon decay and the diagrams of Figs. 4 (c) and 5 (d) when massive vector mesons are involved. In a slightly modified form the diagrams of Fig. 5 are also used to calculate the $\phi \rightarrow S\gamma$ decay [24, 25, 26].

However, the decay amplitude is dominantly characterized by the triangle diagram. The Feynman graphs containing contact vertices arising due to the non-locality only give a minor contribution to the transition amplitude but are required in order to fully restore gauge invariance.

The diagrams are evaluated by applying the technique developed in [17, 18, 19], where each Feynman integral is separated into a part obeying gauge invariance and a remainder term. The remainder terms of each graph cancel each other in total and only the gauge invariant structure of the decay matrix element is left. The matrix element can therefore be written by a linear combination of the form factors $F(p^2, q_1^2, q_2^2)$ and $G(p^2, q_1^2, q_2^2)$ of the respective decay

$$\mathcal{M}^{\mu\nu} = e^2 \left(F(p^2, q_1^2, q_2^2) b^{\mu\nu} + G(p^2, q_1^2, q_2^2) c^{\mu\nu} \right), \quad (20)$$

where the tensor structures are given by

$$\begin{aligned} b^{\mu\nu} &= g^{\mu\nu}(q_1 q_2) - q_1^\mu q_2^\nu \\ c^{\mu\nu} &= g^{\mu\nu} q_1^2 q_2^2 + q_1^\mu q_2^\nu (q_1 q_2) - q_1^\mu q_1^\nu q_2^2 - q_2^\mu q_2^\nu q_1^2. \end{aligned} \quad (21)$$

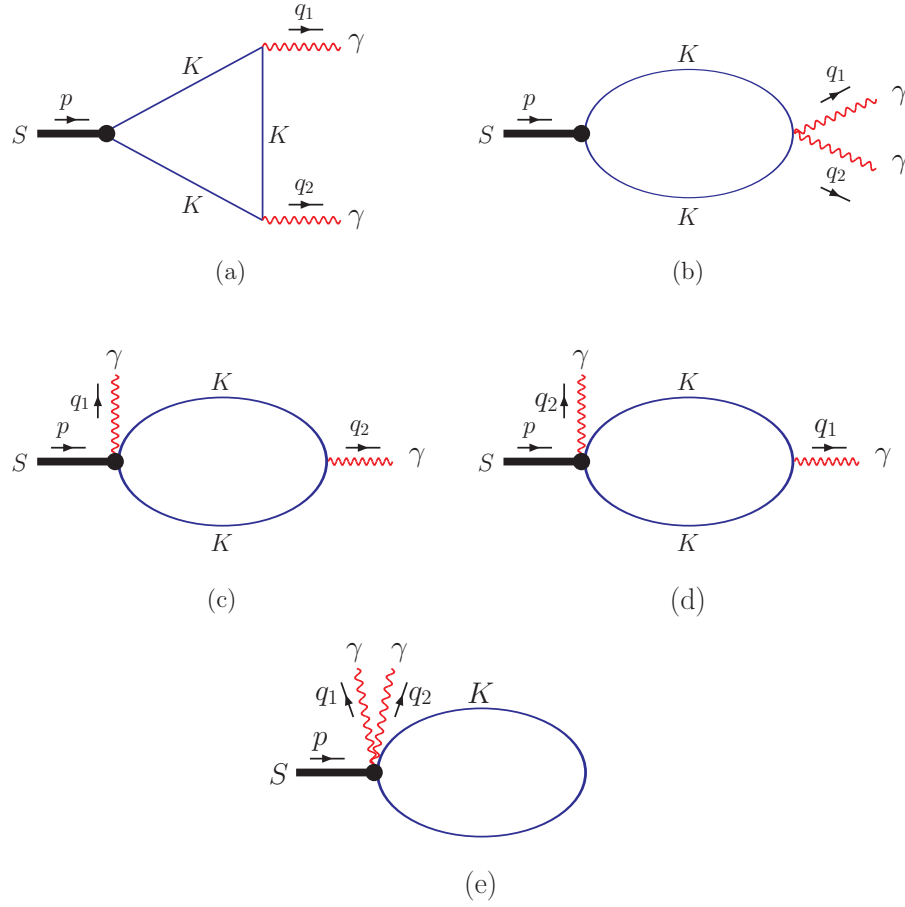


FIG. 3: Diagrams contributing to the electromagnetic $f_0 \rightarrow \gamma\gamma$ and $a_0 \rightarrow \gamma\gamma$ decays.

Here, p and q_1 are the four-momenta of the scalar meson and photon, q_2 is the momentum of the vector meson or second photon depending on the respective decay.

Since in the transition processes we deal with at least one real photon, the second part of $\mathcal{M}^{\mu\nu}$ proportional to $c^{\mu\nu}$ vanishes. The decay constant is therefore characterized by the form factor F which is obtained by evaluating the Feynman integrals for on-shell initial and final states, where $V = \rho, \omega, \phi, \gamma$ represents the vector particle appropriate for the respective decay. In order to allow for $a_0 - f_0$ -mixing, we use $g_{f_0 K^+ K^-}$ and $g_{a_0 K^+ K^-}$ to compute the couplings characterizing the electromagnetic decays

$$\begin{aligned}
 g_{S\gamma\gamma} &\equiv F_{S\gamma\gamma}(m_S^2, 0, 0) = \frac{2}{(4\pi)^2} \cdot \frac{g_{SK^+K^-}}{\sqrt{2}} I_{S\gamma\gamma}(m_S^2, 0, 0) \\
 g_{S\gamma V} &\equiv F_{S\gamma V}(m_S^2, 0, m_V^2) = \frac{1}{(4\pi)^2} g_{VK\bar{K}} g_{SK^+K^-} I_{S\gamma V}(m_S^2, 0, m_V^2) \\
 g_{\phi S\gamma} &\equiv F_{\phi S\gamma}(m_\phi^2, m_S^2, 0) = \frac{1}{(4\pi)^2} g_{\phi K\bar{K}} g_{SK^+K^-} I_{\phi S\gamma}(m_\phi^2, m_S^2, 0),
 \end{aligned} \tag{22}$$

where I denotes the loop integrals and $g_{f_0 K^+ K^-} = \tilde{g}_{f_0 K\bar{K}} \cos\theta - \tilde{g}_{a_0 K\bar{K}} \sin\theta$ and $g_{a_0 K^+ K^-} = \tilde{g}_{a_0 K\bar{K}} \cos\theta + \tilde{g}_{f_0 K\bar{K}} \sin\theta$ (see Eq. 12). The explicit expressions for the loop integrals I are given in Appendix A.

The issue of gauge invariance is considered in more detail in Appendix B and in case of the two-photon decay

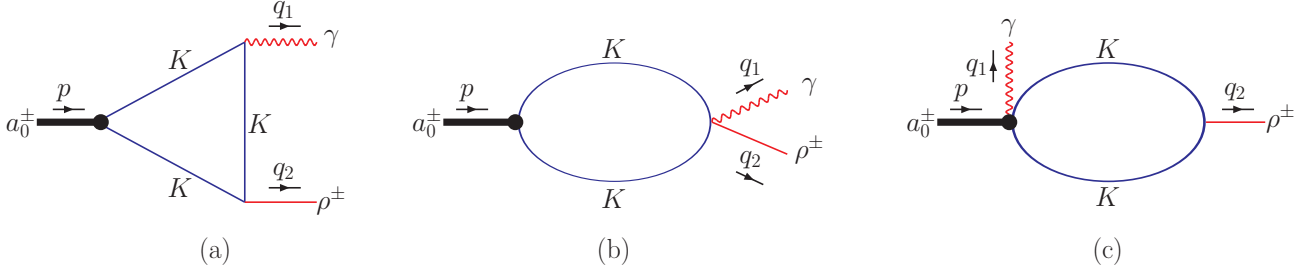


FIG. 4: Diagrams contributing to the charged $a_0^\pm \rightarrow \gamma \rho^\pm$ decay.

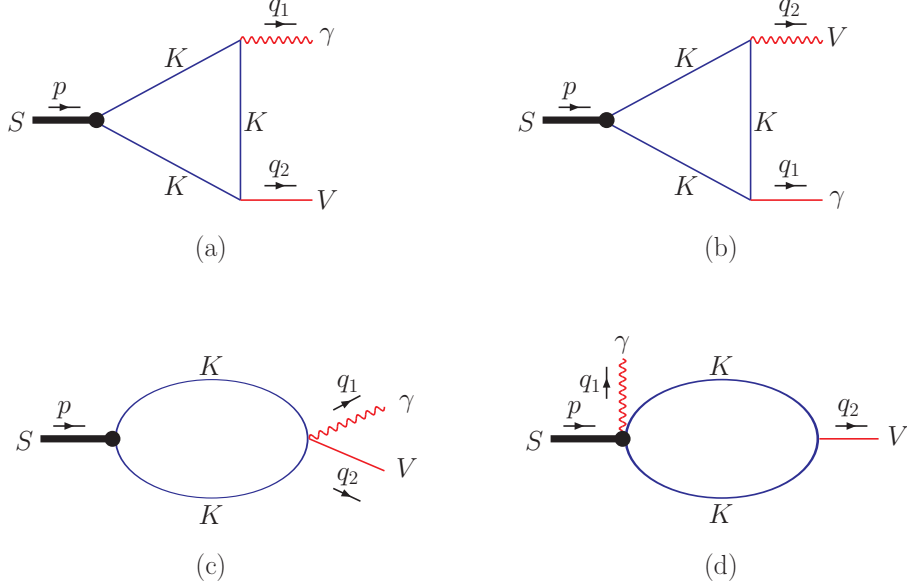


FIG. 5: Diagrams describing the neutral $S \rightarrow \gamma V$ decays ($V = \rho^0, \omega^0$).

in [15, 17].

In [15] we also considered non-trivial $K\bar{K}\gamma$ interaction vertices, where these effects are absorbed in monopole form factors $F_{K\bar{K}\gamma}(Q^2) = \frac{1}{1+Q^2/\Lambda_{K\bar{K}\gamma}^2}$ depending on the photon momentum Q^2 . However, this photon form factor does not influence the decay properties when dealing with real photons as in the present considerations.

IV. STRONG DECAYS

In order to calculate the strong decays of the f_0 and a_0 mesons we proceed in analogy with the computation of the $f_0 \rightarrow \pi\pi$ decay in [15]. In the present paper we extend the formalism by including the $a_0 \rightarrow \pi\eta$ decay and, additionally, by considering mixing between both scalars.

According to the interaction Lagrangians

$$\mathcal{L}_{K^*K\pi} = \frac{g_{K^*K\pi}}{\sqrt{2}} K_\mu^{*\dagger} \vec{\pi} \vec{\tau} i \overleftrightarrow{\partial}^\mu K + h.c., \quad (23)$$

$$\mathcal{L}_{K^*K\eta} = \frac{g_{K^*K\eta}}{\sqrt{2}} K_\mu^{*\dagger} \eta i \overleftrightarrow{\partial}^\mu K + h.c. \quad (24)$$

the strong decays proceed via K^* exchange (see Fig. 6 (a)), where the massive vector meson is described by the anti-symmetric tensor field $W_{\mu\nu} = -W_{\nu\mu}$. Therefore, the phenomenological Lagrangian which generates the contributing

meson-loop diagrams is characterized by the Lagrangian

$$\mathcal{L}_W(x) = -\frac{1}{2} \langle \nabla^\sigma W_{\sigma\mu} \nabla_\nu W^{\nu\mu} + iG_V W_{\mu\nu} [u^\mu u^\nu] \rangle, \quad (25)$$

which involves vector mesons in the tensorial representation [27, 28, 29]. By using low-energy theorems G_V can be expressed through the leptonic decay constant $G_V = F/\sqrt{2}$. The K^* -propagators in vector representation $S_{K^*}^{V;\mu\nu,\alpha\beta}(x)$ and tensorial description $S_{K^*}^{W;\mu\nu,\alpha\beta}(x)$ differ by a term which is reflected in a second diagram containing an explicit four meson vertex (see Fig. 6 (b))

$$S_{K^*}^{W;\mu\nu,\alpha\beta}(x) = S_{K^*}^{V;\mu\nu,\alpha\beta}(x) + \frac{i}{m_{K^*}^2} [g_{\mu\alpha} g_{\nu\beta} - g_{\mu\beta} g_{\nu\alpha}] \delta^4(x). \quad (26)$$

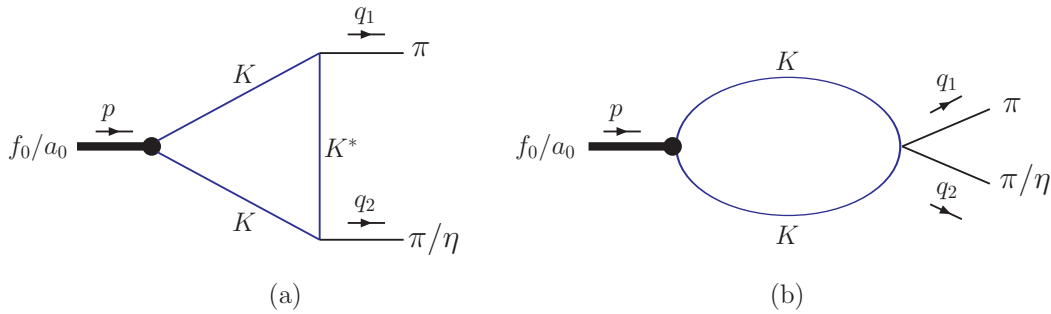


FIG. 6: Diagrams contributing to the strong decays

Graphs describing the strong scalar meson decays are also generated by the Lagrangian of second-order chiral perturbation theory (ChPT) [27, 30]

$$\mathcal{L}_U(x) = \frac{F^2}{4} \langle D_\mu U(x) D^\mu U^\dagger(x) + \chi U^\dagger(x) + \chi^\dagger U(x) \rangle. \quad (27)$$

Here we use the standard notations of ChPT. The fields of pseudoscalar mesons are collected in the chiral matrix $U = u^2 = \exp(i \sum_i \phi_i \lambda_i / F)$ with $F = 92.4$ MeV being the leptonic decay constant and D_μ is the covariant derivative acting on the chiral field. Furthermore $\chi = 2B\mathcal{M} + \dots$, where B is the quark vacuum condensate parameter $B = -\langle 0 | \bar{u}u | 0 \rangle / F^2 = -\langle 0 | \bar{d}d | 0 \rangle / F^2$ and $\mathcal{M} = \text{diag}\{\hat{m}, \hat{m}, m_S\}$ is the mass matrix of current quarks with $\hat{m} = (m_u + m_d)/2$. In the leading order of the chiral expansion the masses of pions and kaons are given by $m_\pi^2 = 2\hat{m}B$, $m_K^2 = (\hat{m} + m_S)B$. In summary, second order ChPT gives rise to a second diagram being of the same structure as graph b) but opposite in sign. Therefore, the triangle diagram a) gives the dominant contribution to the decay amplitude.

The couplings for the strong decays are defined by

$$g_{f_0\pi\pi} = g_{f_0\pi^+\pi^-} = 2g_{f_0\pi^0\pi^0} = G(m_{f_0}^2, m_\pi^2, m_\pi^2) \quad (28)$$

$$g_{a_0\pi\eta} = G(m_{a_0}^2, m_\pi^2, m_\eta^2), \quad (29)$$

where, in the case of the two-pion decay, we have to consider the ratio between the charged and neutral decay modes. Here, $G(p^2, q_1^2, q_2^2)$ is the structure integral of the $f_0 \rightarrow \pi\pi$ and $a_0 \rightarrow \pi\eta$ transitions, which are conventionally split into the two terms $G^{(a)}(p^2, q_1^2, q_2^2)$ and $G^{(b)}(p^2, q_1^2, q_2^2)$. They refer to the contributions of the diagrams of Figs. 6 (a) and 6 (b), respectively, with

$$G(p^2, q_1^2, q_2^2) = G^{(a)}(p^2, q_1^2, q_2^2) + G^{(b)}(p^2, q_1^2, q_2^2). \quad (30)$$

The kaon loop integrals are again expressed in terms of the charged and neutral couplings $g_{SK^+K^-}$ and $g_{SK^0\bar{K}^0}$

$$G(p^2, q_1^2, q_2^2) = \frac{g_{SK^+K^-}}{\sqrt{2}} \cdot I(m_{K^\pm}^2, p^2, q_1^2, q_2^2) + \frac{g_{SK^0\bar{K}^0}}{\sqrt{2}} \cdot I(m_{K^0}^2, p^2, q_1^2, q_2^2), \quad (31)$$

where $I(m_K^2, p^2, q_1^2, q_2^2)$ denotes the contributions from the intermediate charged and neutral kaons.

The expressions for the decay widths are finally given by

$$\Gamma(f_0 \rightarrow \pi\pi) = \Gamma_{f_0\pi^+\pi^-} + \Gamma_{f_0\pi^0\pi^0} = \frac{3}{2}\Gamma_{f_0\pi^+\pi^-} = \frac{3}{32\pi} \frac{g_{f_0\pi\pi}^2}{m_{f_0}} \sqrt{1 - \frac{4m_\pi^2}{m_{f_0}^2}}, \quad (32)$$

$$\Gamma(a_0 \rightarrow \pi\eta) = \frac{1}{16\pi} \frac{g_{a_0\pi\eta}^2}{m_{a_0}} \frac{\lambda^{1/2}(m_{a_0}^2, m_\pi^2, m_\eta^2)}{m_{a_0}^2}, \quad (33)$$

with the Källén-function $\lambda(x, y, z) = x^2 + y^2 + z^2 - 2xy - 2xz - 2yz$.

V. RESULTS

In this section we present our predictions for the electromagnetic and strong decay properties of the scalars f_0 , a_0 and its sensitivity to finite size as well as mixing effects due to isospin violation.

For all the numerical determinations we explicitly use the charged and neutral kaon masses $m_{K^\pm} = 493.677$ MeV and $m_{K^0} = 497.648$ MeV since we consider isospin breaking effects.

The dependence of the nonlocal coupling constants $g_{SK^+K^-}$ and $g_{SK^0\bar{K}^0}$ between the scalars and the charged or neutral constituent kaon pairs on the $a_0 - f_0$ mixing is demonstrated in Fig. 7. We plot the coupling constants for the size parameter $\Lambda = 1$ GeV as functions of the mixing angle θ .

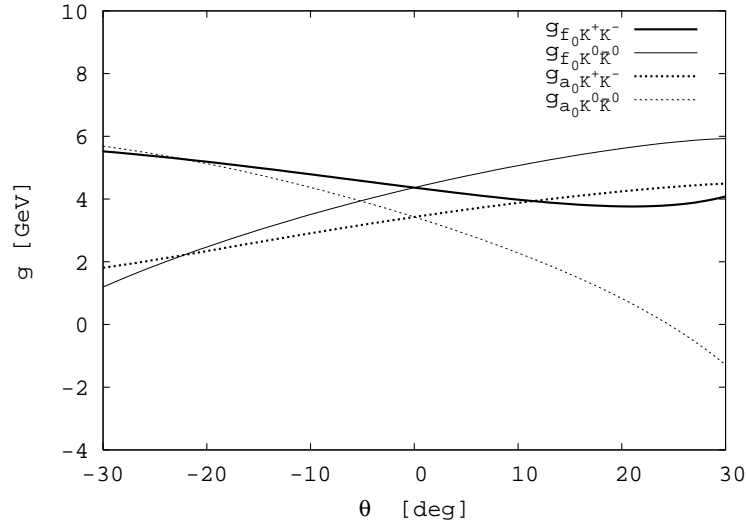


FIG. 7: Influence of mixing effects on the couplings $g_{f_0 K^+ K^-}$ ($g_{f_0 K^0 \bar{K}^0}$) and $g_{a_0 K^+ K^-}$ ($g_{a_0 K^0 \bar{K}^0}$) at $\Lambda = 1$ GeV.

Without mixing ($\theta = 0$) we obtain for the nonlocal and local couplings $g_{SK\bar{K}} \equiv g_{SK^+K^-} = g_{SK^0\bar{K}^0}$ the explicit values of

$$\begin{aligned} \frac{g_{f_0 K\bar{K};L}}{\sqrt{2}} &= 2.90 \text{ GeV (local)}, & \frac{g_{f_0 K\bar{K}}}{\sqrt{2}} &= 3.09 \text{ GeV } (\Lambda = 1 \text{ GeV}), \\ \frac{g_{a_0 K\bar{K};L}}{\sqrt{2}} &= 2.32 \text{ GeV (local)}, & \frac{g_{a_0 K\bar{K}}}{\sqrt{2}} &= 2.42 \text{ GeV } (\Lambda = 1 \text{ GeV}). \end{aligned} \quad (34)$$

For the computation of the radiative decay properties we use the vector meson masses quoted in [31]

$$\begin{aligned} m_\rho &= 0.7755 \text{ GeV}, \\ m_\omega &= 0.78265 \text{ GeV}, \\ m_\phi &= 1.02 \text{ GeV}. \end{aligned} \quad (35)$$

The respective coupling constants are taken from [32] in which $SU(3)$ symmetry relations are used to fix $g_{VK\bar{K}} = g_{\rho K\bar{K}} = g_{\omega K\bar{K}} = 4.24$ and $g_{\phi K\bar{K}} = 6$.

The expressions for the electromagnetic decay widths are given by

$$\begin{aligned}\Gamma_{S\gamma\gamma} &= \frac{\alpha^2\pi}{4}m_S^3g_{S\gamma\gamma}^2, \\ \Gamma_{S\gamma\rho/\omega} &= \frac{\alpha}{8}\frac{(m_S^2 - m_\rho^2)^3}{m_S^3}g_{S\gamma\rho/\omega}^2, \\ \Gamma_{\phi S\gamma} &= \frac{\alpha}{24}\frac{(m_\phi^2 - m_S^2)^3}{m_S^3}g_{\phi S\gamma}^2,\end{aligned}\tag{36}$$

where the coupling constants describing the radiative decays are related to the form factor F as described in (22). In Appendix C our full results for the radiative decays of the neutral scalars a_0^0 and f_0 are collected in Tabs. VII and VIII for different mixing angles θ . The first value of each column is related to the nonlocal case with the size parameter $\Lambda = 1$ GeV, the second entry denotes the decay properties in the local limit. For simplicity the calculations for the ϕ -decay are restricted to the local limit. The predictions for the decay properties in Tables VII and VIII obviously show that an isospin violating mixture can only be realized for small mixing angles θ . In summary we quote the results for the $f_0 \rightarrow \gamma\gamma$ decay when θ is varied between -3° and 3° :

$$\begin{aligned}\Gamma(f_0 \rightarrow \gamma\gamma) &= 0.28 \text{ keV} - 0.31 \text{ keV (local)}, \\ \Gamma(f_0 \rightarrow \gamma\gamma) &= 0.23 \text{ keV} - 0.26 \text{ keV } (\Lambda = 1 \text{ GeV}).\end{aligned}\tag{37}$$

The sensitivity of the $f_0 \rightarrow \gamma\gamma$ decay properties on finite size effects has been intensely studied in [15], even in case of virtual photons, and leads to a variation of $\Gamma(f_0 \rightarrow \gamma\gamma)$ from

$$\Gamma(f_0 \rightarrow \gamma\gamma) = 0.21 \text{ keV } (\Lambda = 0.7 \text{ GeV}) - 0.26 \text{ keV } (\Lambda = 1.3 \text{ GeV})\tag{38}$$

for $\theta = 0^\circ$. In Tables I and II we draw the comparison with data and other approaches, respectively. The $f_0 \rightarrow \gamma\gamma$ width predicted by our model matches the range of values currently deduced by experiment.

TABLE I: Electromagnetic decay width $f_0(980) \rightarrow \gamma\gamma$: experimental data.

Experiment	[31]	[33]	[34]	[35]
$\Gamma(f_0 \rightarrow \gamma\gamma)$ [keV]	$0.29_{-0.09}^{+0.07}$	$0.205_{-0.083}^{+0.095} +_{-0.117}^{+0.147}$	$0.31 \pm 0.14 \pm 0.09$	$0.29 \pm 0.07 \pm 0.12$

TABLE II: Electromagnetic decay width $f_0(980) \rightarrow \gamma\gamma$: theoretical approaches.

Reference	[21]	[36]	[37]	[38]	[6]	[39]	[10]
Meson structure	$(q\bar{q})$	$(q\bar{q})$	$(q\bar{q})$	$(q\bar{q})$	$(q^2\bar{q}^2)$	(hadronic)	(hadronic)
$\Gamma(f_0 \rightarrow \gamma\gamma)$ [keV]	0.24	$0.28_{-0.13}^{+0.09}$	0.31	0.33	0.27	0.20	0.22 ± 0.07

For the two-photon decay of the a_0 meson our results lie between

$$\begin{aligned}\Gamma(a_0 \rightarrow \gamma\gamma) &= 0.21 \text{ keV} - 0.25 \text{ keV (local)}, \\ \Gamma(a_0 \rightarrow \gamma\gamma) &= 0.17 \text{ keV} - 0.21 \text{ keV } (\Lambda = 1 \text{ GeV}),\end{aligned}\tag{39}$$

where again θ lies within the small interval from -3° to 3° . For positive mixing angles our predictions are in good agreement with the experimental result 0.3 ± 0.1 keV measured by Crystal Barrel [40]. Finite size effects play a comparable role as $a_0 - f_0$ mixing since the variation of Λ from 0.7 GeV to 1.3 GeV changes $\Gamma(a_0 \rightarrow \gamma\gamma)$ by

$$\Gamma(a_0 \rightarrow \gamma\gamma) = 0.16 \text{ keV } (\Lambda = 0.7 \text{ GeV}) - 0.21 \text{ keV } (\Lambda = 1.3 \text{ GeV}),\tag{40}$$

where $\theta = 0^\circ$. The decay widths obtained in other approaches are combined in Tab. III and show a large discrepancy even for models with the same structure assumptions.

TABLE III: Electromagnetic decay width $a_0(980) \rightarrow \gamma\gamma$: theoretical approaches.

Reference	[36]	[41]	[6]	[39]
Meson structure	$(q\bar{q})$	$(q\bar{q})$	$(q^2\bar{q}^2)$	(hadronic)
$\Gamma(a_0 \rightarrow \gamma\gamma)$ [keV]	$0.3^{+0.11}_{-0.10}$	1.5	0.27	0.78

The radiative ϕ decay widths calculated in the local limit within the framework of our formalism lie within the range

$$\begin{aligned}\Gamma(\phi \rightarrow f_0\gamma) &= 0.54 \text{ keV} - 0.61 \text{ keV}, \\ \Gamma(\phi \rightarrow a_0\gamma) &= 0.31 \text{ keV} - 0.36 \text{ keV}.\end{aligned}\tag{41}$$

Our results are close to the branching ratios quoted by PDG (2007) [31]: The ratios $\Gamma(\phi \rightarrow a_0\gamma)/\Gamma_{total} = (0.76 \pm 0.06) \cdot 10^{-4}$ and $\Gamma(\phi \rightarrow f_0\gamma)/\Gamma_{total} = (1.11 \pm 0.07) \cdot 10^{-4}$ give 0.32 keV for the $\phi \rightarrow a_0\gamma$ decay width and an upper limit of 0.51 keV for $\Gamma(\phi \rightarrow f_0\gamma)$, respectively. Due to the self-consistent determination of the $g_{a_0 K \bar{K}}$ coupling constant our result in case of the a_0 production is smaller than the width $\Gamma(\phi \rightarrow a_0\gamma)$ quoted in [11, 25], but have quite good agreement with the predictions for the ϕ -production of the f_0 .

For the decays involving ρ and ω mesons we predict:

$$\begin{aligned}\Gamma(f_0 \rightarrow \rho\gamma) &= 7.61 - 8.60 \text{ keV (local)} & \text{and} & & 7.17 - 8.04 \text{ keV } (\Lambda = 1 \text{ GeV}), \\ \Gamma(f_0 \rightarrow \omega\gamma) &= 7.12 - 8.06 \text{ keV (local)} & \text{and} & & 6.73 - 7.55 \text{ keV } (\Lambda = 1 \text{ GeV}), \\ \Gamma(a_0 \rightarrow \rho\gamma) &= 6.57 - 7.81 \text{ keV (local)} & \text{and} & & 6.03 - 7.16 \text{ keV } (\Lambda = 1 \text{ GeV}), \\ \Gamma(a_0 \rightarrow \omega\gamma) &= 6.18 - 7.35 \text{ keV (local)} & \text{and} & & 5.69 - 6.75 \text{ keV } (\Lambda = 1 \text{ GeV}).\end{aligned}\tag{42}$$

The deviations from the predicted widths of Ref. [11] for the $a_0/f_0 \rightarrow \gamma\rho/\omega$ decays arise because of different assumptions for the scalar masses and couplings. In [42] the decay width $a_0 \rightarrow \gamma\rho/\omega$ calculated within the framework of a Chiral Unitarity Approach is larger than our result because of the additional inclusion of vector mesons in the loop diagrams.

In summary, by restricting to small mixing angles our results for the electromagnetic f_0 and a_0 decay properties are in quite good agreement with present experimental data. Therefore, the hadronic molecule approach is suitable to describe radiative f_0 and a_0 decays. However, other structure components besides the $K\bar{K}$ configuration can possibly be realized. Therefore, current data do not allow any definite and final conclusion concerning the substructure of the scalar mesons since calculations based on other approaches give similar results and even overlap with each other as demonstrated in Tables II and III.

A further step forward would be a more precise experimental determination of the decay properties but also of the mixing angle θ to shed light on the isospin violating mixing mechanisms. A possible access to the mixing angle θ is given by the ratio between charged and neutral scalar a_0 meson decays since the coupling to the charged a_0^\pm mesons is not affected by mixing.

In the numerical computations of the strong $f_0 \rightarrow \pi\pi$ and $a_0 \rightarrow \pi\eta$ decays we restrict to the charged pion mass ($m_\pi \equiv m_{\pi^\pm} 139.57 \text{ MeV}$) but consider explicit kaon masses $m_{K^0} \neq m_{K^\pm}$. Assuming $\Lambda = 1 \text{ GeV}$ we obtain the results listed in Tab. IX. When varying θ between -3° and 3° the width $\Gamma(f_0 \rightarrow \pi\pi)$ lies in the range of values

$$\Gamma(f_0 \rightarrow \pi\pi) = 55.7 \text{ MeV} - 58.9 \text{ MeV},\tag{43}$$

consistent with the experimental data listed in Tab. IV.

TABLE IV: Strong decay width $f_0(980) \rightarrow \pi\pi$: experimental data.

Data	PDG [31]	BELLE [33]	[43]
$\Gamma(f_0 \rightarrow \pi\pi)$ [MeV]	40 - 100	$51.3^{+20.8+13.2}_{-17.7-3.8}$	80 ± 10

Further theoretical predictions are indicated in Tab. V which, unfortunately, cover a large range of values, even

TABLE V: Strong decay width $f_0(980) \rightarrow \pi\pi$: theoretical approaches.

Reference	[21]	[44]	[45]	[37]	[46]	[47]
Meson structure	$q\bar{q}$	$q\bar{q}$	$q\bar{q}$	$q\bar{q}$	$q\bar{q}$	hadronic
$\Gamma(f_0 \rightarrow \pi\pi)$ [MeV]	20	28	52-58	53	56	18.2

for the same structure assumption. Again, the present situation for $\Gamma(f_0 \rightarrow \pi\pi)$ does not allow for a clear statement concerning the f_0 structure.

For the strong $a_0 \rightarrow \pi\eta$ decay we obtain

$$\Gamma(a_0 \rightarrow \pi\eta) = 58.9 \text{ MeV} - 63.4 \text{ MeV} \quad (44)$$

with $\theta \in [-3^\circ, 3^\circ]$, which also matches with the experimental results listed in Tab. VI. Here, the quarkonium models of [41] and [37] clearly deliver larger results compared to the molecular interpretation and data.

TABLE VI: Strong decay width $a_0(980) \rightarrow \pi\eta$: data and theoretical approaches.

Reference	[31]	[48]	[49]	[41]	[37]
	experimental data			$q\bar{q}$	$q\bar{q}$
$\Gamma(f_0 \rightarrow \pi\eta)$ [MeV]	50-100	$50 \pm 13 \pm 4$	61 ± 19	225	138

VI. SUMMARY

The radiative decay properties of the a_0 and f_0 mesons have been comprehensively studied within a model which is covariant and obeys full gauge invariance with respect to the electromagnetic interaction. The present framework, where the scalars are assumed to be hadronic $K\bar{K}$ molecules, provides a straightforward and consistent determination of the decay properties, in particular the coupling constants and decay widths. The coupling to the constituent kaons including f_0 - a_0 mixing effects have been determined by the compositeness condition which reduces the number of free parameters to the size parameter Λ and the mixing angle θ .

Our results for the electromagnetic decays ($a_0/f_0 \rightarrow \gamma\gamma$ and $\phi \rightarrow \gamma a_0/f_0$) and, in addition, the strong decay widths ($f_0 \rightarrow \pi\pi$ and $a_0 \rightarrow \pi\eta$) are analyzed with respect to f_0 - a_0 mixing effects and finite size effects.

We come to the conclusion that the hadronic molecule interpretation is sufficient to describe both the electromagnetic and strong a_0 and f_0 decays, based on the current status of experimental data. Furthermore, the $a_0 - f_0$ mixing angle could be determined by a precise measurement of the ratio of the charged and neutral a_0 meson decays. The $f_0 - a_0$ mixing strength could deliver new insights into the contributions being responsible for isospin-violating mixing and the meson structure issue.

Acknowledgments

This work was supported by the DFG under contracts FA67/31-1 and GRK683. This research is also part of the EU Integrated Infrastructure Initiative Hadronphysics project under contract number RII3-CT-2004-506078 and President grant of Russia ‘‘Scientific Schools’’ No. 817.2008.2.

APPENDIX A: LOOP INTEGRALS

Here we give a short presentation of the structure integrals and its evaluation relevant for the derivation of the transition form factors. For simplicity we restrict to the diagrams of Figs. 3 (a,b), 4 (a,b) and 5 (a) to (c), which do not contain contact vertices. The additional diagrams generated due to nonlocal effects are discussed in detail in [15, 17]. The full structure integrals characterizing the electromagnetic decays are given by

$$I_{S\gamma V}^{\mu\nu}(m_S^2, 0, m_V^2) = \int \frac{d^4 k}{\pi^2 i} \tilde{\Phi}(-k^2) \left((2k+p-q)^\mu (2k-q)^\nu S_K(k+\frac{p}{2}) S_K(k-\frac{p}{2}) S_K(k+\frac{p}{2}-q) + g^{\mu\nu} S_K(k+\frac{p}{2}) S_K(k-\frac{p}{2}) \right), \quad (\text{A1})$$

$$I_{\phi S\gamma}^{\mu\nu}(m_\phi^2, m_S^2, 0) = \int \frac{d^4 k}{\pi^2 i} \tilde{\Phi}(-k^2) \left(\frac{(2k-q-p)^\nu (2k-q)^\mu}{S_K(k+\frac{p}{2}) S_K(k-\frac{p}{2}) S_K(k-\frac{p}{2}-q)} + \frac{g^{\mu\nu}}{S_K(k+\frac{p}{2}) S_K(k-\frac{p}{2})} \right),$$

where q is the photon momentum and p of the scalar. In the case of the two-photon decay the expressions corresponding to all the diagrams of Fig. 3 are quoted in [15]. We use the expression for the $S \rightarrow V\gamma$ decay (Eq. A1) as an example to demonstrate the technique for the derivation of the loop integral $I_{S\gamma V}(m_S^2, 0, m_V^2)$. In the first step we separate the gauge invariant part of the full expression $I^{\mu\nu}$ by writing

$$I_{S\gamma V}^{\mu\nu}(m_S^2, 0, m_V^2) = I_{S\gamma V}(m_S^2, 0, m_V^2) b^{\mu\nu} + I_{S\gamma V}^{(2)}(m_S^2, 0, m_V^2) c^{\mu\nu} + \delta I_{S\gamma V}, \quad (\text{A2})$$

where the remainder term $\delta I_{S\gamma V}$ contains the non-invariant terms. The tensor structures $b^{\mu\nu}$ and $c^{\mu\nu}$ have already been defined in (21). Since we deal with real photons, only the first term of (A2), proportional to $b^{\mu\nu}$, is relevant. In the second step Feynman-parametrization is introduced the integration over the four-momentum k is performed. For instance, in the local limit we obtain

$$I_{S\gamma V}(m_S^2, 0, m_V) = \int_0^1 d^3 \alpha \delta(1 - \sum_i \alpha_i) \frac{4\alpha_1 \alpha_3}{m_K^2 - m_S^2 \alpha_1 \alpha_3 - m_V^2 \alpha_2 \alpha_3}. \quad (\text{A3})$$

The mathematical treatment of the diagrams including contact vertices is straightforward and in complete analogy with above example.

The loop integrals of the diagrams contributing to the strong decays (Fig. 6 (a) and (b)) read as

$$I^{(a)}(m_K^2, p^2, q_1^2, q_2^2) = \frac{g_\pi g_{\pi(\eta)}}{(4\pi)^2} \int \frac{d^4 k}{\pi^2 i} \tilde{\Phi}(-k^2) (k - \frac{p}{2} - q_2)_\mu (k + \frac{p}{2} + q_1)_\nu S_K(k + \frac{p}{2}) S_K(k - \frac{p}{2}) S_{K^*}^{\mu\nu}(k + \frac{p}{2} - q_1),$$

$$I^{(b)}(m_K^2, p^2, q_1^2, q_2^2) = -\frac{1}{m_{K^*}^2} \frac{g_\pi g_{\pi(\eta)}}{(4\pi)^2} \int \frac{d^4 k}{\pi^2 i} \tilde{\Phi}(-k^2) (k - \frac{p}{2} - q_2)(k + \frac{p}{2} + q_1) S_K(k + \frac{p}{2}) S_K(k - \frac{p}{2}). \quad (\text{A4})$$

Again, we evaluate above expressions by introducing Feynman parameters and integrating over the loop-momentum k .

APPENDIX B: GAUGE INVARIANCE

In this appendix gauge invariance is demonstrated by means of the charged a_0 meson decays. The kaon loop integral corresponding to the diagrams (a) and (b) of Fig. 4 is given by

$$I_\Delta^{\mu\nu} = \int \frac{d^4 k}{\pi^2 i} \tilde{\Phi}(-k^2) \left\{ S(k + \frac{p}{2}) S(k - \frac{q}{2}) S(k - \frac{p}{2}) (2k + q_2)^\mu (2k - q_1)^\nu + g^{\mu\nu} S(k + \frac{p}{2}) S(k - \frac{p}{2}) \right\}, \quad (\text{B1})$$

where $q = q_1 - q_2$. The part $I_\Delta^{\mu\nu}$ being gauge invariant with respect to the photon momentum q_1^μ is separated from the so-called remainder term $\delta I_\Delta^{\mu\nu}$ by using

$$(2k + q_2)^\mu = (2k + q_2)_{\perp q_1}^\mu + q_1 (2k + q_2) \frac{q_1^\mu}{q_1^2}$$

$$g^{\mu\nu} = g_{\perp q_1}^{\mu\nu} + \frac{q_1^\mu q_1^\nu}{q_1^2}. \quad (\text{B2})$$

Therefore, the non-invariant term is given by

$$\begin{aligned}
\delta I_{\Delta}^{\mu\nu} &= \int \frac{d^4 k}{\pi^2 i} \tilde{\Phi}(-k^2) \left\{ \left[S\left(k + \frac{p}{2}\right) S\left(k - \frac{p}{2}\right) - S\left(k - \frac{p}{2}\right) S\left(k - \frac{q}{2}\right) \right] \frac{q_1^\mu}{q_1^2} (2k - q_1)^\nu \right. \\
&\quad \left. + S\left(k + \frac{p}{2}\right) S\left(k - \frac{p}{2}\right) \frac{q_1^\mu q_1^\nu}{q_1^2} \right\} \\
&= - \int \frac{d^4 k}{\pi^2 i} \tilde{\Phi}(-k^2) S\left(k - \frac{p}{2}\right) S\left(k - \frac{q}{2}\right) \frac{q_1^\mu}{q_1^2} (2k - q_1)^\nu.
\end{aligned} \tag{B3}$$

For the bubble diagram (c) of Fig. 4 the loop integral reads as (see [17])

$$I_{bub}^{\mu\nu} = - \int \frac{d^4 k}{\pi^2 i} (2k + \frac{q_1}{2})^\mu k^\nu \int_0^1 dt \tilde{\Phi}' \left[- \left(k + \frac{q_1}{2}\right)^2 t - k^2 (1-t) \right]. \tag{B4}$$

This leads to the remainder

$$\delta I_{bub}^{\mu\nu} = \int \frac{d^4 k}{\pi^2 i} \tilde{\Phi}(-k^2) \frac{q_1^\mu}{q_1^2} (2k - q_1)^\nu S\left(k - \frac{p}{2}\right) S\left(k - \frac{q}{2}\right) \tag{B5}$$

which cancels with $\delta I_{\Delta}^{\mu\nu}$ and therefore

$$\delta I^{\mu\nu} = \delta I_{\Delta}^{\mu\nu} + \delta I_{bub}^{\mu\nu} = 0. \tag{B6}$$

APPENDIX C: SUMMARY TABLES

For completeness we indicate in the following tables the full list of couplings and transition widths for an $a_0 - f_0$ mixing angle θ with $-3^\circ \leq \theta \leq 45^\circ$.

TABLE VII: f_0 decay properties for different mixing angles θ (first value of each column refers to nonlocal ($\Lambda = 1$ GeV), second local case).

θ	$g_{f_0\gamma\gamma}$ [MeV ⁻¹]		$\Gamma_{f_0\gamma\gamma}$ [keV]		$g_{f_0\rho\gamma}$ [GeV ⁻¹]		$\Gamma_{f_0\rho\gamma}$ [keV]		$g_{f_0\omega\gamma}$ [GeV ⁻¹]		$\Gamma_{f_0\omega\gamma}$ [keV]		$g_{\phi f_0\gamma}$ [GeV ⁻¹]	$\Gamma_{\phi f_0\gamma}$ [keV]
-3°	81.33	88.98	0.26	0.31	0.42	0.44	8.04	8.60	0.43	0.44	7.55	8.06	2.03	0.61
-2°	80.56	88.08	0.26	0.31	0.42	0.43	7.89	8.43	0.43	0.44	7.40	7.90	2.01	0.59
-1°	79.79	87.19	0.25	0.30	0.42	0.43	7.74	8.26	0.42	0.44	7.26	7.74	1.99	0.58
0°	79.03	86.30	0.25	0.29	0.41	0.42	7.59	8.10	0.42	0.43	7.13	7.58	1.97	0.57
1°	78.28	85.42	0.24	0.29	0.41	0.42	7.45	7.93	0.41	0.43	6.99	7.43	1.95	0.56
2°	77.54	84.54	0.24	0.28	0.40	0.42	7.31	7.77	0.41	0.42	6.86	7.27	1.93	0.55
3°	76.80	83.67	0.23	0.28	0.40	0.41	7.17	7.61	0.41	0.42	6.73	7.12	1.91	0.54
5°	75.37	81.96	0.22	0.26	0.39	0.40	6.90	7.30	0.40	0.41	6.48	6.84	1.87	0.51
10°	72.09	77.96	0.20	0.24	0.38	0.38	6.31	6.61	0.38	0.39	5.93	6.19	1.78	0.46
20°	68.20	72.55	0.18	0.21	0.35	0.36	5.65	5.72	0.36	0.36	5.31	5.36	1.66	0.40
45°	133.73	141.32	0.70	0.79	0.70	0.70	21.73	21.71	0.71	0.71	20.40	20.33	3.23	1.53

TABLE VIII: a_0 decay properties for different mixing angles θ (first value of each column refers to the nonlocal ($\Lambda = 1$ GeV), second local case).

θ	$g_{a_0\gamma\gamma}$ [MeV $^{-1}$]		$\Gamma_{a_0\gamma\gamma}$ [keV]		$g_{a_0\rho\gamma}$ [GeV $^{-1}$]		$\Gamma_{a_0\rho\gamma}$ [keV]		$g_{a_0\omega\gamma}$ [GeV $^{-1}$]		$\Gamma_{a_0\omega\gamma}$ [keV]		$g_{\phi a_0\gamma}$ [GeV $^{-1}$]	$\Gamma_{\phi a_0\gamma}$ [keV]
-3°	66.10	72.75	0.17	0.21	0.36	0.37	6.03	6.57	0.36	0.38	5.69	6.18	1.74	0.31
-2°	67.12	73.89	0.18	0.22	0.36	0.38	6.22	6.78	0.37	0.38	5.87	6.38	1.76	0.32
-1°	68.12	75.01	0.19	0.22	0.37	0.38	6.41	6.98	0.37	0.39	6.05	6.57	1.79	0.33
0°	69.11	76.11	0.19	0.23	0.37	0.39	6.60	7.19	0.38	0.39	6.22	6.77	1.82	0.33
1°	70.08	77.20	0.20	0.24	0.38	0.39	6.78	7.40	0.38	0.40	6.40	6.96	1.84	0.34
2°	71.04	78.26	0.20	0.24	0.38	0.40	6.97	7.60	0.39	0.41	6.58	7.15	1.87	0.35
3°	71.98	79.31	0.21	0.25	0.39	0.40	7.16	7.81	0.39	0.41	6.75	7.35	1.89	0.36
5°	73.83	81.36	0.22	0.26	0.40	0.41	7.53	8.21	0.40	0.42	7.10	7.73	1.94	0.38
10°	78.15	86.14	0.24	0.30	0.42	0.44	8.44	9.21	0.43	0.45	7.96	8.67	2.05	0.43
20°	85.56	94.19	0.29	0.35	0.46	0.48	10.11	11.01	0.47	0.49	9.54	10.36	2.25	0.51
45°	62.60	65.54	0.16	0.17	0.34	0.33	5.41	5.33	0.34	0.34	5.11	5.017	1.56	0.25

TABLE IX: Strong a_0 and f_0 decay properties in dependence on θ ($\Lambda = 1$ GeV).

θ	-3°	-2°	-1°	0°	1°	2°	3°	5°	10°	20°	45°
$g_{f_0\pi\pi}$ [GeV]	1.38	1.39	1.40	1.40	1.41	1.41	1.42	1.43	1.46	1.52	1.66
$\Gamma_{f_0\pi\pi}$ [MeV]	55.71	56.28	56.83	57.37	57.90	58.41	58.91	59.88	62.18	67.18	80.43
$g_{a_0\pi\eta}$ [GeV]	2.19	2.18	2.17	2.16	2.14	2.13	2.11	2.08	1.98	1.69	-1.06
$\Gamma_{a_0\pi\eta}$ [MeV]	63.39	62.74	62.05	61.33	60.56	59.74	58.89	57.05	51.72	37.61	14.84

-
- [1] N. A. Tornqvist, Z. Phys. C **68**, 647 (1995) [arXiv:hep-ph/9504372].
[2] E. van Beveren and G. Rupp, Eur. Phys. J. C **10**, 469 (1999) [arXiv:hep-ph/9806246].
[3] F. Giacosa, arXiv:0804.3216 [hep-ph]; F. Giacosa, Phys. Rev. D **75**, 054007 (2007) [arXiv:hep-ph/0611388].
[4] F. Giacosa, Phys. Rev. D **74**, 014028 (2006) [arXiv:hep-ph/0605191].
[5] R. L. Jaffe, Phys. Rev. D **15**, 267 (1977).
[6] N. N. Achasov, S. A. Devyanin and G. N. Shestakov, Phys. Lett. B **108**, 134 (1982) [Erratum-ibid. B **108**, 435 (1982)].
[7] D. Black, M. Harada and J. Schechter, Prog. Theor. Phys. Suppl. **168**, 173 (2007) [arXiv:0705.0802 [hep-ph]].
[8] A. H. Fariborz, R. Jora and J. Schechter, Phys. Rev. D **76**, 014011 (2007) [arXiv:hep-ph/0612200].
[9] J. D. Weinstein and N. Isgur, Phys. Rev. Lett. **48**, 659 (1982); Phys. Rev. D **27**, 588 (1983); Phys. Rev. D **41**, 2236 (1990).
[10] C. Hanhart, Yu. S. Kalashnikova, A. E. Kudryavtsev and A. V. Nefediev, Phys. Rev. D **75**, 074015 (2007) [arXiv:hep-ph/0701214].
[11] Yu. Kalashnikova, A. E. Kudryavtsev, A. V. Nefediev, J. Haidenbauer and C. Hanhart, Phys. Rev. C **73**, 045203 (2006) [arXiv:nucl-th/0512028].
[12] F. E. Close and A. Kirk, Phys. Lett. B **489**, 24 (2000) [arXiv:hep-ph/0008066].
[13] C. Hanhart, B. Kubis and J. R. Pelaez, Phys. Rev. D **76**, 074028 (2007) [arXiv:0707.0262 [hep-ph]].

- [14] N. N. Achasov and A. V. Kiselev, Phys. Lett. B **534**, 83 (2002) [arXiv:hep-ph/0203042]; N. N. Achasov and G. N. Shestakov, Phys. Rev. D **70**, 074015 (2004) [arXiv:hep-ph/0405129].
- [15] T. Branz, T. Gutsche and V. E. Lyubovitskij, arXiv:0712.0354 [hep-ph] Eur. Phys. J. A (in print).
- [16] I. V. Anikin, M. A. Ivanov, N. B. Kulimanova and V. E. Lyubovitskij, Z. Phys. C **65**, 681 (1995); M. A. Ivanov, M. P. Locher and V. E. Lyubovitskij, Few Body Syst. **21**, 131 (1996); M. A. Ivanov, V. E. Lyubovitskij, J. G. Körner and P. Kroll, Phys. Rev. D **56**, 348 (1997) [arXiv:hep-ph/9612463].
- [17] A. Faessler, T. Gutsche, M. A. Ivanov, V. E. Lyubovitskij and P. Wang, Phys. Rev. D **68**, 014011 (2003) [arXiv:hep-ph/0304031].
- [18] A. Faessler, T. Gutsche, M. A. Ivanov, J. G. Körner and V. E. Lyubovitskij, Phys. Lett. B **518**, 55 (2001) [arXiv:hep-ph/0107205]; A. Faessler, T. Gutsche, M. A. Ivanov, J. G. Korner, V. E. Lyubovitskij, D. Nicmorus and K. Pumsa-ard, Phys. Rev. D **73**, 094013 (2006) [arXiv:hep-ph/0602193]; A. Faessler, T. Gutsche, B. R. Holstein, V. E. Lyubovitskij, D. Nicmorus and K. Pumsa-ard, Phys. Rev. D **74**, 074010 (2006) [arXiv:hep-ph/0608015].
- [19] A. Faessler, T. Gutsche, V. E. Lyubovitskij and Y. L. Ma, Phys. Rev. D **76**, 014005 (2007) [arXiv:0705.0254 [hep-ph]]; A. Faessler, T. Gutsche, V. E. Lyubovitskij and Y. L. Ma, arXiv:0709.3946 [hep-ph]; A. Faessler, T. Gutsche, V. E. Lyubovitskij and Y. L. Ma, Phys. Rev. D **77**, 114013 (2008) [arXiv:0801.2232 [hep-ph]]; Y. B. Dong, A. Faessler, T. Gutsche and V. E. Lyubovitskij, Phys. Rev. D **77**, 094013 (2008) [arXiv:0802.3610 [hep-ph]]; A. Faessler, T. Gutsche, V. E. Lyubovitskij and Y. L. Ma, Phys. Rev. D **76**, 114008 (2007) [arXiv:0709.3946 [hep-ph]]; A. Faessler, T. Gutsche, S. Kovalenko and V. E. Lyubovitskij, Phys. Rev. D **76**, 014003 (2007) [arXiv:0705.0892 [hep-ph]].
- [20] S. Weinberg, Phys. Rev. **130**, 776 (1963).
- [21] G. V. Efimov and M. A. Ivanov, *The Quark Confinement Model of Hadrons*, (IOP Publishing, Bristol & Philadelphia, 1993).
- [22] V. Baru, J. Haidenbauer, C. Hanhart, Yu. Kalashnikova and A. E. Kudryavtsev, Phys. Lett. B **586**, 53 (2004) [arXiv:hep-ph/0308129].
- [23] J. Terning, Phys. Rev. D **44**, 887 (1991).
- [24] Yu. S. Kalashnikova, A. E. Kudryavtsev, A. V. Nefediev, C. Hanhart and J. Haidenbauer, Eur. Phys. J. A **24**, 437 (2005) [arXiv:hep-ph/0412340].
- [25] F. E. Close, N. Isgur and S. Kumano, Nucl. Phys. B **389**, 513 (1993) [arXiv:hep-ph/9301253].
- [26] J. A. Oller, Nucl. Phys. A **714**, 161 (2003) [arXiv:hep-ph/0205121].
- [27] J. Gasser and H. Leutwyler, Annals Phys. **158**, 142 (1984).
- [28] G. Ecker, J. Gasser, H. Leutwyler, A. Pich and E. de Rafael, Phys. Lett. B **223**, 425 (1989).
- [29] G. Ecker, J. Gasser, A. Pich and E. de Rafael, Nucl. Phys. B **321**, 311 (1989).
- [30] S. Weinberg, Physica A **96**, 327 (1979).
- [31] W. M. Yao *et al.* [Particle Data Group], J. Phys. G **33**, 1 (2006).
- [32] Y. J. Zhang, H. C. Chiang, P. N. Shen and B. S. Zou, Phys. Rev. D **74**, 014013 (2006) [arXiv:hep-ph/0604271].
- [33] T. Mori *et al.* [Belle Collaboration], Phys. Rev. D **75**, 051101 (2007) [arXiv:hep-ex/0610038].
- [34] H. Marsiske *et al.* [Crystal Ball Collaboration], Phys. Rev. D **41**, 3324 (1990).
- [35] J. Boyer *et al.*, Phys. Rev. D **42**, 1350 (1990).
- [36] A. V. Anisovich, V. V. Anisovich and V. A. Nikonov, Eur. Phys. J. A **12**, 103 (2001) [arXiv:hep-ph/0108186].
- [37] M. D. Scadron, G. Rupp, F. Kleefeld and E. van Beveren, Phys. Rev. D **69**, 014010 (2004) [Erratum-ibid. D **69**, 059901 (2004)] [arXiv:hep-ph/0309109].
- [38] M. Schumacher, Eur. Phys. J. A **30**, 413 (2006) [Erratum-ibid. A **32**, 121 (2007)] [arXiv:hep-ph/0609040].
- [39] J. A. Oller and E. Oset, Nucl. Phys. A **629**, 739 (1998) [arXiv:hep-ph/9706487].
- [40] C. Amsler, Rev. Mod. Phys. **70**, 1293 (1998) [arXiv:hep-ex/9708025].
- [41] T. Barnes, Phys. Lett. B **165**, 434 (1985).
- [42] H. Nagahiro, L. Roca and E. Oset, Eur. Phys. J. A **36**, 73 (2008) [arXiv:0802.0455 [hep-ph]].
- [43] D. Barberis *et al.* [WA102 Collaboration], Phys. Lett. B **453**, 316 (1999) [arXiv:hep-ex/9903043].
- [44] M. K. Volkov and V. L. Yudichev, Phys. Atom. Nucl. **64**, 2006 (2001) [Yad. Fiz. **64**, 2091 (2001)] [arXiv:hep-ph/0011326].
- [45] V. V. Anisovich and A. V. Sarantsev, Eur. Phys. J. A **16**, 229 (2003) [arXiv:hep-ph/0204328].
- [46] L. S. Celenza, S. f. Gao, B. Huang, H. Wang and C. M. Shakin, Phys. Rev. C **61**, 035201 (2000).
- [47] J. A. Oller, E. Oset and J. R. Pelaez, Phys. Rev. D **59**, 074001 (1999) [Erratum-ibid. D **60**, 099906 (1999), Erratum-ibid. D **75**, 099903 (2007)] [arXiv:hep-ph/9804209].
- [48] P. Achard *et al.* [L3 Collaboration], Phys. Lett. B **526**, 269 (2002) [arXiv:hep-ex/0110073].
- [49] D. Barberis *et al.* [WA102 Collaboration], Phys. Lett. B **488**, 225 (2000) [arXiv:hep-ex/0007019].